MOLECULAR PHYSICS, 1973, VOL. 25, NO. 1, 193–209

Kinetics of the triplet state of 2,3-dichloroquinoxaline from microwave-induced phosphorescence transients

by D. SCHWEITZER†, J. ZUCLICH‡, and A. H. MAKI
Department of Chemistry, University of California, Riverside, California 92502

(*Received* 19 *June* 1972)

The phosphorescent state of 2,3-dichloroquinoxaline doped into single crystals of durene and 1,2,4,5-tetrachlorobenzene has been studied using several methods based upon optical detection of magnetic resonance (ODMR). Flash excitation and continuous optical pumping methods are described and analysed. Phosphorescent transient effects caused by spin-lattice relaxation and variable intersystem crossing rates are observed and described using first-order solutions of the appropriate rate equations. The effects of spatial polarization of the phosphorescence (anisotropic spatial distribution of phosphorescence intensity) of single crystals on ODMR signals is observed and discussed. The spatial polarization of emission can cause difficulties in determining relative radiative rate constants of the triplet sublevels in oriented samples, but can yield information about the linear polarization of the emission analogous to that obtained by conventional means using polarizers.

1. INTRODUCTION

Optical detection of magnetic resonance (ODMR) has proven to be a versatile technique for the investigation of the dynamic properties of the phosphorescent states of organic molecules. Sharnoff [1] and Kwiram [2] first used ODMR for the detection of microwave transitions betweens the Zeeman levels of the triplet state of aromatic hydrocarbons in a magnetic field. Schmidt and van der Waals extended ODMR to the study of zero-field transitions of aza-aromatic triplet states [3]. A short time later, Tinti *et al.* [4, 5] reported a phosphorescence-microwave double-resonance (PDMR) experiment at zero-field in which ODMR effects were observed on individual vibronic bands of the phosphorescence emission. These experiments led to the optical detection of ENDOR [6] and EEDOR [7] in organic triplet states. The static methods mentioned above yield detailed information about the energy level structure of the phosphorescent state, but no quantitative information about its dynamic features, i.e. the decay constants of the individual triplet sublevels, the relative radiative rate constants, the relative populating rate constants, and spin-lattice relaxation rate constants. Dynamic information of a quantitative nature may be obtained from experiments such as microwave-induced delayed phosphorescence [8, 9], optical detection of adiabatic inversion [10, 11] and, more recently, the analysis of phosphorescence transients which follow a saturating fast-passage [12].

† On leave from the Max Planck Institute, Department of Molecular Physics, Heidelberg, Germany.

‡ U.S. Public Health Service Postdoctoral Fellow.

The problem of spin-lattice relaxation has hampered the interpretation of a great deal of data concerning the triplet state dynamics, and investigators have typically sought to achieve sample temperatures which are sufficiently low that spin-lattice relaxation can be neglected in relation to the decay rates of the triplet sublevels. In many cases, however, the data are found to be still influenced by spin-lattice relaxation, even at the lowest temperatures achieved in pumped-helium experiments (1·1–1·2 K) [13].

Another complicating feature which has received little attention in the interpretation of PMDR experiments on single crystal samples is the spatial polarization of the phosphorescence emission. If the phosphorescence emission is of mixed polarization, the relative intensity of vibronic bands of different polarization generally will depend on the orientation of the crystal relative to the viewing direction. The same applies to the relative intensity of the emission originating from different spin sublevels if both are radiative in the same vibronic band.

In this communication, we describe the application of some of the methods mentioned above to an analysis of the dynamics of the phosphorescent state of 2,3-dichloroquinoxaline incorporated into host crystals of durene and *sym*-tetrachlorobenzene. Also, we describe the results of experiments in which the triplet state is populated by flash excitation, rather than by continuous optical pumping.

We have observed microwave induced transient effects on the phosphorescence emission which are due to spin-lattice relaxation, and to changes in the intersystem crossing rates caused by the depletion of the ground singlet state. These effects are compared qualitatively with first-order solutions of the appropriate rate equations.

We consider, also, the effects of the spatial polarization of the emission, which are particularly striking in 2,3-dichloroquinoxaline whose emission is of mixed polarization.

2. Phosphorescence spectra

2.1. *Radiative selection rules for 2,3-dichloroquinoxaline*

The radiative selection rules for 2,3-dichloroquinoxaline have been described by Tinti and El-Sayed [14] using group theoretical methods with the assumption of C_{2v} molecular symmetry. Figure 1 (*a*) gives the energy level diagram and defines the important rate constants involving the triplet sublevels. The polarizations of the electric dipole transitions from the individual zero-field levels to the vibronic levels of the electronic ground state are shown in figure 1 (*b*) [14]. The solid lines are transitions which obtain their intensity by spin-orbit mixing between the triplet and singlet states which differ in the orbital type of one electron (e.g., S_{σ,π^*} and T_{π,π^*}) while the dashed lines represent transitions whose intensity arises from mixing between states of the same electronic type (S_{π,π^*} and T_{π,π^*}). The latter type transitions are expected to be weaker in aromatic molecules. The dash-dot transition gains its intensity from a spin-vibronic perturbation which is not expected to be very efficient. If we assume the following mechanism for the vibronic activity of the $^3B_2$ state of 2,3-dichloroquinoxaline,

$$^3B_2 \xleftrightsquigarrow{\mathscr{H}_{\text{vib}}} {}^3(n, \pi^*) \xleftrightsquigarrow{\mathscr{H}_{\text{so}}} {}^1(\pi, \pi^*),$$

then the intermediate triplet is $^3B_1$ for emission to vibronic levels of a_2 symmetry, and $^3A_2$ for emission to vibronic levels of b_1 symmetry. Both T_y and T_z may in principle emit to vibronic levels of a_2 and b_1 symmetry from group theory arguments. The vibronic coupling is the same for T_y and T_z but these spin sublevels are coupled to different $^1(\pi, \pi^*)$ states by the y- and z-components of the spin-orbit coupling hamiltonian, respectively. Differences in radiative intensity from

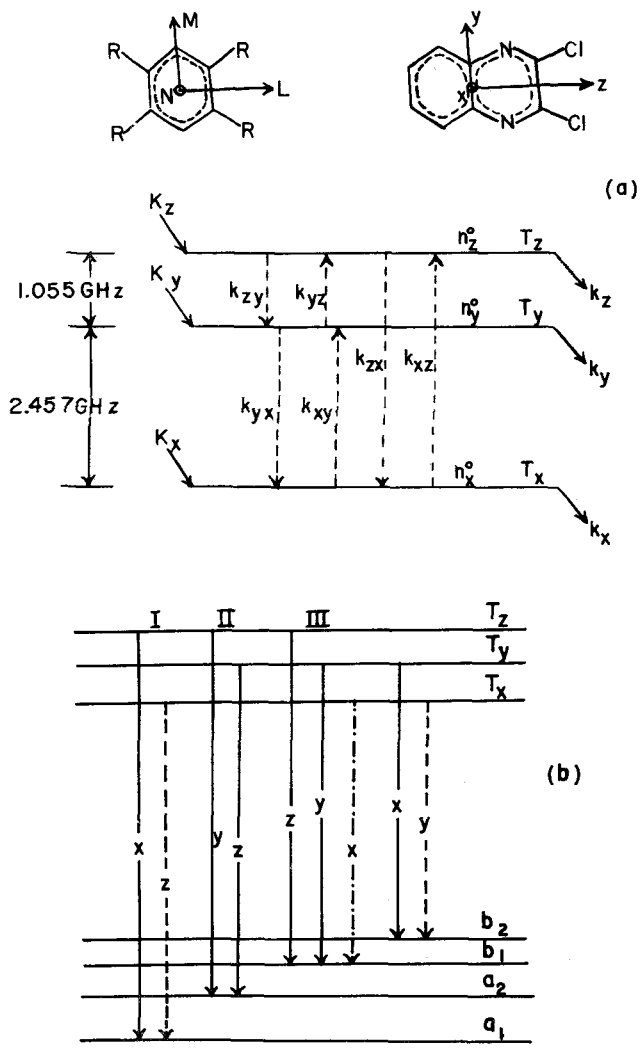

Figure 1. (*a*) coordinate system and zero-field triplet sublevel energy diagram of 2,3-dichloroquinoxaline. Intersystem crossing, spin-lattice relaxation, and individual sublevel decay constants are indicated. (*b*) radiative decay pathways of 1,2-dichloroquinoxaline ($^3B_2$, π, π^*) to ground singlet ($^1A_1$) vibronic states in C_{2v} symmetry. Predicted polarization of the electric dipole transition moment is indicated. Solid line transitions occur through spin-orbit coupling between $^3(\pi, \pi^*)$ and $^1(\sigma, \pi^*)$ states, while dashed-line transitions occur through spin-orbit mixing between $^3(\pi, \pi^*)$ and $^1(\pi, \pi^*)$ states. The dashed-dot transition requires a spin-vibronic perturbation in addition to spin-orbit coupling between $^3(\pi, \pi^*)$ and $^1(\sigma, \pi^*)$ states. Roman numerals refer to transition types defined in text and in [14].

the T_y and T_z sublevels should reflect the relative magnitudes of the pertinent spin-orbit coupling matrix elements, although they will also depend to some extent on energy gaps and the oscillator strengths of the $S_0 \leftarrow {}^1(\pi, \pi^*)$ transitions from which they derive their intensity.

2.2. *Spatial polarization of the phosphorescence*

In addition to being linearly polarized along a molecular axis, the radiation emitted by an excited molecule is also spatially polarized. The radiation is emitted preferentially along the plane normal to the axis of polarization. We would then expect the relative intensity of different vibronic bands in the luminescence spectrum of a single crystal sample to depend upon the crystal axis along which the radiation is collected, if the polarization of the emission is different in different vibronic bands. The details of the variation in relative intensity depend upon the crystal structure of the sample. In their analysis of the phosphorescence spectrum of 2,3-dichloroquinoxaline, Tinti and El-Sayed [14] distinguished three different types of bands. Type I bands require only spin-orbit perturbation ; the emission originates entirely from T_z and is polarized along the molecular x-direction. The 0,0-band is of this type, as well as transitions to other totally symmetric vibronic levels. Type II bands originate solely from the T_y level gaining intensity from a spin-orbit-vibronic perturbation involving an a_2 vibration. The 0,0–262 cm^{-1} band is an example of a Type II band. The emission is z-polarized. Type III bands are of mixed polarization ; the emission originates from T_y and T_z and is also allowed by a spin-orbit-vibronic perturbation. The band at 0, 0–490 cm^{-1} in durene is an example of a Type III band requiring a b_1 vibration. The emission from T_y and T_z are y- and z-polarized, respectively.

In discussing the spatial polarization of the phosphorescence spectrum of 2,3-dichloroquinoxaline in durene, and 1,2,4,5-tetrachlorobenzene host crystals, we must first have a look at the structures of these hosts.

2.2.1. *Durene host crystal*

The arrangement of the molecules of a durene crystal in the unit cell is given by Hutchison and Mangum [15]. The durene crystal is monoclinic with

$$a = 11{\cdot}57 \pm 0{\cdot}05 \text{ Å}, \quad b = 5{\cdot}77 \pm 0{\cdot}02 \text{ Å}, \quad c = 7{\cdot}03 \pm 0{\cdot}05 \text{ Å}, \quad \beta = 113{\cdot}3°.$$

There are two durene molecules per unit cell, each with its M-axis nearly perpendicular to the 010-plane. The two molecules are related by a two-fold screw rotation about the b-axis. The angles which relate the molecular L- and N-axes to the a, b, and c' axes of the crystal are given in references [15] and [16]. If we assume that in the crystal which is doped with 2,3-dichloroquinoxaline, the x, y, and z-axes (figure 1 (a)) are oriented in the directions of the durene N-,M-, and L-axes, respectively, the relative orientation of the x, y, and z-axes of the inequivalent 2,3-dichloroquinoxaline molecules are determined by the durene unit cell [15, 16]. The y-axes of both molecules are oriented nearly along the durene b-axis, and the respective z-axes are nearly perpendicular to one another. It is apparent that because of the relative orientation of the two sites, x- and z-polarized emission will have the same spatial polarization. If the emission of 2,3-dichloroquinoxaline can be described in terms of Type I, II and III bands, the relative intensities of Type I, Type II, and the z-polarized components of the Type III bands should be

invariant with direction, while the relative intensity of the y-polarized component of Type III bands (originating from T_y) will vary. The latter emission will have a minimum intensity along the crystal b-axis.

2.2.2. *1,2,4,5-tetrachlorobenzene host crystal*

The crystal structure of 1,2,4,5-tetrachlorobenzene is given by Dean *et al.* [17] who found the crystal to be monoclinic with $a = 3{\cdot}85 \pm 0{\cdot}005$ Å, $b = 10{\cdot}602 \pm 0{\cdot}005$ Å, $c = 9{\cdot}725 \pm 0{\cdot}005$ Å and $\beta = 103{\cdot}28°$. The unit cell contains two molecules with their N-axes parallel to the crystal a-axis. The molecules lie in the bc′ crystal plane with the L-axis of one site parallel to the M-axis of the other. If we assume that the 2,3-dichloroquinoxaline molecules enter the crystal substitutionally with the molecular x-, y-, and z-axes parallel to N-, M-, and L-, respectively, the inequivalent 2,3-dichloroquinoxaline molecules have their x-axes parallel, and oriented along the a-axis, while the molecular yz planes lie in the crystal bc' plane with the z-axis of one normal to the z-axis of the other. A phase transition to a triclinic structure [18] which occurs on cooling below 188 K results in only very small changes in the molecular orientations. In this crystal, the spatial polarization of Type I bands is unique with minimum intensity along the crystal a-axis. The intensity of Type I bands will vary relative to Type II and both components of Type III.

2.3. *Experimental*

Crystals of 2,3-dichloroquinoxaline in durene and in 1,2,4,5-tetrachlorobenzene were prepared by several recrystallizations and zone refining of the pure components (*circa* 300 passes). The components were melted together *in vacuo* and single crystals were grown by the Bridgeman method, and annealed at 5°C below their respective melting points for a period of several days followed by gradual cooling to room temperature over a period of 24 hours. The extent of doping was about 10^{-3}–10^{-4} mol/mol. For measurements of the phosphorescence spectra, samples were oriented in a liquid He dewar and their temperature reduced to 1·2–1·3 K by pumping. The crystals were excited with a PEK 100W mercury lamp filtered with a $\frac{1}{4}$-meter Bausch and Lomb Monochromator. An excitation band between 3060 and 3120 Å was selected. The phosphorescence was monitored at right-angles to the excitation path with a McPherson Model 2051 one meter grating monochromator using narrow slits (between 50μ/50μ and 120μ/120μ, 0·8–2 Å bandwidth). Phosphorescence was detected using a cooled EMI Model 9558QA Photomultiplier.

Microwave-induced phosphorescence transients were measured as described previously [12]. For the flash-excitation measurements, the mercury lamp and $\frac{1}{4}$-meter monochromator were replaced by a Chadwick–Helmuth, Inc. Model 135 N/1 source using a PEK X–80 xenon lamp. The exciting light was filtered through an aqueous $NiSO_4$ solution and Corning 7–54 glass filter. Signal averaging was generally employed.

2.4. *Results*

The low temperature phosphorescence spectrum of 2,3-dichloroquinoxaline in durene has been described in some detail in [14]. The directional dependence of the spectrum was not discussed, however. Figures 2 (*a*) and (*c*) show part of

the phosphorescence spectrum of 2,3-dichloroquinoxaline in durene at 1·3 K. The crystal was mounted so that it could be rotated about the *a*-crystal axis, with the viewing direction normal to *a*. The spectrum observed in figure 2 (*c*) is from the crystal after rotation of 90° relative to the orientation of figure 2 (*a*). No polarizer is used in these experiments. There is no change observed in the relative intensity of the 0,0 and 0,0–262 cm^{-1} bands, which is consistent with their assignment as Type I and II bands, respectively. We do observe, however, a large

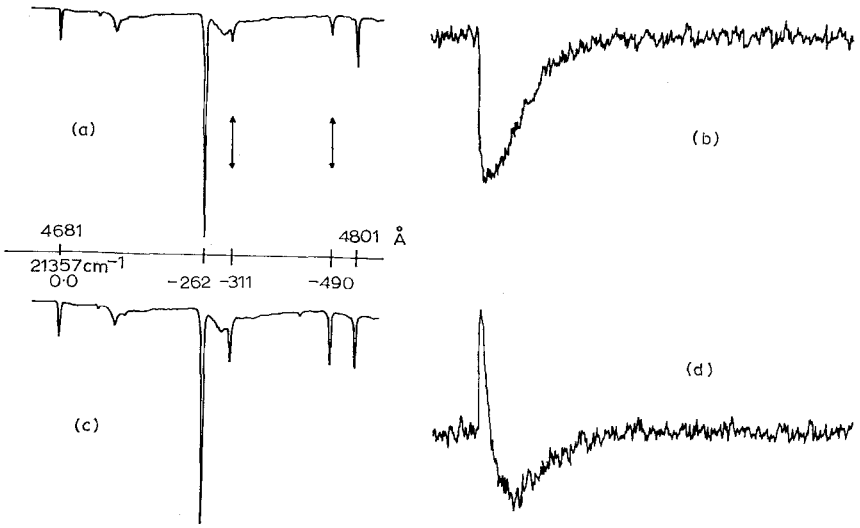

Figure 2. Phosphorescence spectra of 2,3-dichloroquinoxaline in durene at $T=1·3$ K in two differing crystal orientations and phosphorescence transients induced in the 0,0–490 cm^{-1} emission band on saturation of the 1·055 GHz ($T_y \leftrightarrow T_z$) microwave transition. (*a*) and (*b*) correspond to one orientation, while (*c*) and (*d*) correspond to the other. All signals correspond to uncorrected photomultiplier output. Emission signals are thus downward.

change in the intensity of the bands at 0,0–311 cm^{-1}, and 0,0–490 cm^{-1} relative to the previously mentioned bands. These bands must have a *y*-polarized component, consistent with their assignment as Type III bands. In a later section we will describe the influence of the different space polarization of the T_y and T_z emissions of Type III bands on the observed phosphorescence transients induced by microwave fast-passage. Figure 3 shows the emission of 2,3-dichloroquinoxaline in the tetrachlorobenzene host for two different orientations of the crystal. In the lower spectrum, the crystal is rotated by 60° about the *b*-axis relative to the upper spectrum. The viewing direction is normal to the *b*-axis. As expected, we observed a large change in the relative intensities of the 0,0 (Type I) and the 0,0–267 cm^{-1} (Type II) bands. The band labelled *X* in figure 3 is the origin of a 2,3-dichloroquinoxaline triplet which apparently occupies a different lattice site. The band labelled *X*–267 is a Type II vibronic band of this minor site. ODMR measurements monitoring the emission of the *X*–267 cm^{-1} band gives signals at microwave frequencies which are shifted about 100 MHz from those of the major emitting species.

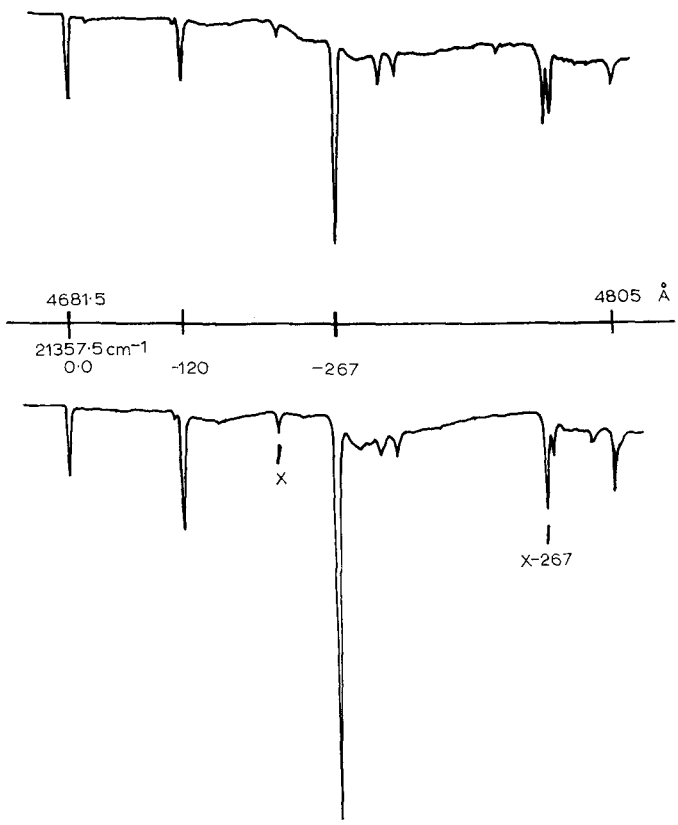

Figure 3. Phosphorescence emission of 2,3-dichloroquinoxaline in 1,2,4,5-tetrachlorobenzene at 1·3 K in two different crystal orientations. See text for details.

3. Phosphorescence decay—microwave fast-passage experiments

3.1. *Discussion of the methods*

In this section we describe experiments done on 2,3-dichloroquinoxaline doped into single crystals of durene in which the guest triplet is populated by a single intense flash from a high pressure xenon flashlamp. The decay of the phosphorescence emission is monitored in a single vibronic band using a high-resolution monochromator-photomultiplier combination. The effects of one or more saturating microwave fast-passages on the decay curve of the phosphorescence are accumulated using signal averaging techniques. ODMR measurements following flashlamp excitation were reported first by Antheunis *et al.* [9], and more recently by El-Sayed and Olmsted [19]. The major advantage of flash excitation of the triplet state is that if the duration of the flash is short compared with the reciprocal of the sublevel decay rates and spin-lattice relaxation (SLR) rates the sublevel populations at the end of the flash are proportional to their respective intersystem crossing (ISC) rates. Microwave saturation of populations after a time interval which is short compared with the inverse decay rates and SLR rates can be used to obtain the relative ISC rates directly. The relative ISC rates follow from steady-state optical pumping experiments only if the SLR rates are negligible. The population of the

uth triplet sublevel immediately following a flash of short duration compared with the decay times and the SLR times is given by

$$n_u' = n_a K_u, \tag{1}$$

where n_a is a constant depending upon experimental conditions and K_u is the ISC rate constant for populating the T_u sublevel. The subsequent decay of the population of the uth sublevel is given by the solution of three coupled differential equations, a representative of which is

$$dn_u/dt = \rho_u' n_u + k_{vu} n_v + k_{wu} n_w, \tag{2}$$

where $\rho_u' = k_u + k_{uv} + k_{uw}$. The solutions for the decay of the populations following the flash may be obtained readily to first order under the assumption that

$$k_{vu} < |\rho_u' - \rho_v'|.$$

Each sublevel decays as the sum of three exponentials. We find in first order that

$$n_u^{(1)} = n_a \left\{ K_u \exp(-\rho_u' t) + \sum_v{}' [K_v k_{vu}/(\rho_u' - \rho_v')] \right. \\ \left. [\exp(-\rho_v' t) - \exp(-\rho_u' t)] \right\}. \tag{3}$$

The decay of n_u is a simple exponential with rate constant ρ_u' if either K_v, $K_w = 0$, or if k_{vu}, $k_{wu} = 0$. In an experiment in which the population of a pair of levels (T_u and T_v) are kept saturated by microwaves during the light flash, or are saturated after a time interval which is short compared with the decay times, the decay of the population of the uth level after saturation is given by equation (3) above, but with K_u and K_v each replaced with $(K_u + K_v)/2$.

3.2. *Results*

The decay of the 0,0–262 cm^{-1} emission following the flash at 1·3 K is shown in figure 4 (*c*). It is a simple exponential decay with a decay constant of 143 msec (1/e value). Previous work [14] has indicated that the emission in the 0,0–262 cm^{-1} band originates principally from T_y. Similarly [14], $K_y \gg K_x, K_z$. This is consistent with our failure to observe deviations from a simple exponential decay. At 4·2 K, a simple exponential decay of 120 msec is observed. We attribute the reduced lifetime to an increase in k_{yz} and/or k_{yx}. The corresponding values are reported as $\rho_y'^{-1}$ in the table. The effect at 1·3 K of saturating the $T_y \leftrightarrow T_x$ transition on the emission is shown in figure 4 (*d*). The emission is cut approximately in half after saturation, and decays with a lifetime characteristic of the T_y level. No long-lived emission tail is detected after saturation of $T_y \leftrightarrow T_x$; the T_x level is not radiative in the 0,0–262 cm^{-1} band as far as we can detect. We obtained the lifetime of the T_x level by a double microwave fast-passage experiment. The first microwave saturating passage was carried out as just described. After a time interval sufficiently long that the emission from T_y was gone, the $T_y \leftrightarrow T_x$ transition was again saturated, and the amplitude of the induced phosphorescent spike recorded. A plot of the amplitude versus the time interval between saturating passages exhibits a good exponential decay which we interpret

as $\rho_x'^{-1}$. The values are given at 1·3 and 4·2 K in the table. The large difference in life-times at these two temperatures indicates that spin-lattice relaxation effects are important in determining the life-time of the long-lived T_x sublevel.

The decay of the 0,0-band emission following the flash is shown in figure 4 (*a*). The decay is non-exponential, but it can be resolved into two exponential decays. The longer of the decay constants is 2·5 s at 1·3 K, the same as $\rho_x'^{-1}$ at this temperature. The shorter of the decay constants is 234 msec at 1·3 K. It is known

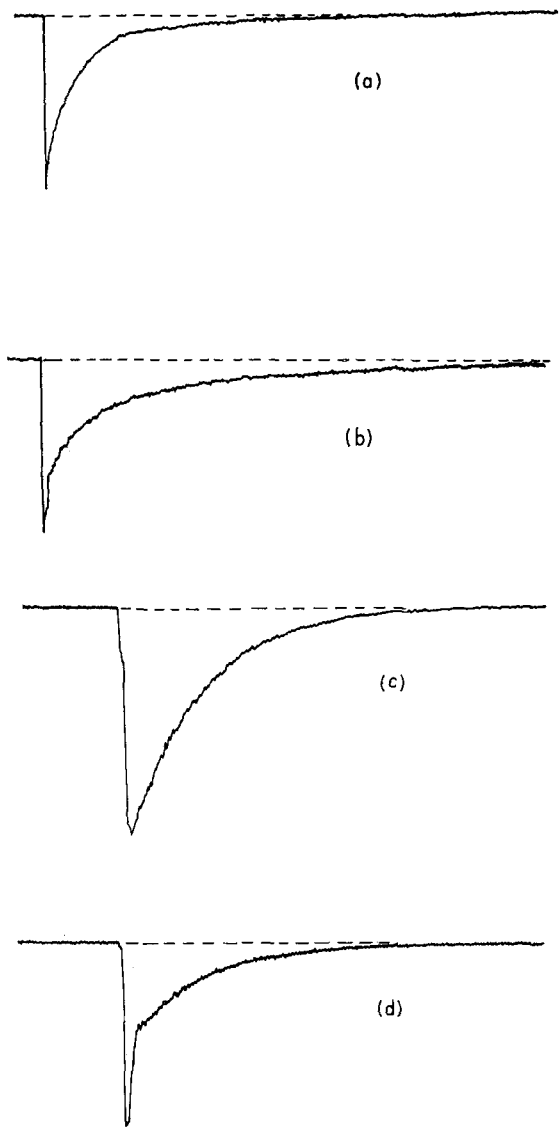

Figure 4. (*a*) Decay of 0,0–band emission of 2,3-dichloroquinoxaline in durene at 1·3 K following flash excitation. (*b*) Decay of 0,0–band emission following flash and microwave saturation of the 2·457 GHz ($T_y \leftrightarrow T_x$) transition. (*c*) Decay of the 0,0–262 cm^{-1} phosphorescence after flash excitation. (*d*) Decay of the 0,0–262 cm^{-1} emission following flash and saturation of the 2·457 GHz ($T_y \leftrightarrow T_x$) transition. Emission increases downwards.

from earlier work [14] that emission in the 0,0–band originates primarily from the T_z sublevel. Immediately after the flash, however, the triplet population is almost all in the T_y sublevel [14], and a small radiative decay rate from T_y cannot be ignored. If the $T_y \leftrightarrow T_z$ (1·055 GHz) transition is saturated a few millisec after the flash, we find a sudden approximately fourfold increase in the emission intensity and a decay constant of 285 msec, a significantly longer decay than was found for the fast component of the 0,0–band decay in the absence of microwave saturation.

Sublevel	$\rho_u'(\text{sec}^{-1})$†	n_u^0(per cent)‡	p_u(per cent)§	p_u/ρ_u'(per cent)‖
T_x	0·40 (0·67)	38·9 (33)	7·5	55·8
T_y	6·90 (8·33)	47·1 (51)	82·2	35·4
T_z	3·50 (4·35)	14·0 (16)	10·3	8·8

† Total decay constant. Values at $T=1{\cdot}3$ K; bracketed values at $T=4{\cdot}2$ K.

‡ Steady-state population. Obtained from microwave-induced phosphorescence transients during cw optical pumping, $T=1{\cdot}3$ K. Bracketed values at 4·2 K.

§ Relative ISC rates. Obtained from flash excitation experiments at 1·3 K.

‖ Predicted n_u^0 in absence of SLR.

Properties of the sublevels of the 2,3-dichloroquinoxaline triplet.

We interpret the decay which follows the microwave saturation as $\rho_z'^{-1}$. Apparently, the fast component of the decay following the flash is not a simple exponential decay, although we could not resolve it into the expected ρ_z' and ρ_y' decays.

The emission from T_z for short times following the flash varies as

$$I_{0,z} \cong n_a k_{z,0}^{(r)}(\mathbf{p}) \left[\left(K_z + \frac{K_y k_{yz}}{(\rho_y' - \rho_z')} \right) \exp(-\rho_z' t) - \frac{K_y k_{yz}}{(\rho_y' - \rho_z')} \exp(-\rho_y' t) \right], \qquad (3\,a)$$

whereas, the emission from T_y is principally

$$I_{0,y} \simeq n_a k_{y,0}^{(r)}(\mathbf{p}) K_y \exp(-\rho_y' t). \qquad (3\,b)$$

Here, $k_{u,0}^{(r)}(\mathbf{p})$ is the radiative rate constant for 0,0-emission of T_u along the observation direction represented by the vector $\mathbf{p}$. If $k_{y,0}^{(r)}(\mathbf{p})=0$, the decay of the 0,0-band emission would be given by (3 *a*) above, and since $\rho_y' > \rho_z'$, the second term in the brackets due to SLR from T_y would effectively *lengthen* the observed lifetime of T_z. Our observation of a shortened lifetime can be explained only by emission from T_y according to equation (3 *b*). We can conclude that

$$k_{y,0}^{(r)}(\mathbf{p})/k_{z,0}^{(r)}(\mathbf{p}) > k_{yz}/(\rho_y' - \rho_z') \qquad (3\,c)$$

at 1·3 K. The long tail is due either to T_x emission in the 0,0–band, to T_z emission fed by SLR from the T_x sublevel, or to a combination of both. A large enhancement of the emission intensity of the long-lived component is found if the $T_y \leftrightarrow T_x$

transition is saturated shortly after the flash (figure 4 (*b*)). Since almost the entire population of the triplet is in T_y after the flash, saturation of the $T_y \leftrightarrow T_x$ transition corresponds to transfer of approximately one half of the entire triplet population from T_y to T_x. The sudden decrease of the intensity of the 0,0-emission upon saturation of the T_y and T_x sublevels again shows that $k_{y,0}{}^{(r)}(\mathbf{p}) > k_{x,0}{}^{(r)}(\mathbf{p})$.

The relative ISC rates, K_x, K_y, and K_z, as well as the ratio $k_{y,0}{}^{(r)}(\mathbf{p})/k_{z,0}{}^{(r)}(\mathbf{p})$ were obtained from the flash experiments in which the 0–0-band emission was monitored, and each of the three microwave transitions was saturated shortly after the flash. It was assumed that $k_{x,0}{}^{(r)}(\mathbf{p}) = 0$. Evidence for this assumption is presented in the following section. The relative ISC rates are given in the table. In the particular crystal orientation of these experiments $k_{y,0}{}^{(r)}(\mathbf{p})/k_{z,0}{}^{(r)}(\mathbf{p}) = 0{\cdot}057$ It then follows from equation (3 *c*) that $k_{yz} < 0{\cdot}19$ sec^{-1} at 1·3 K.

4. Phosphorescence transients induced by microwave fast-passage

4.1. *Discussion of the method*

In a previous communication [12] it was shown that kinetic information about the triplet state could be obtained from an analysis of the phosphorescence transient induced by a saturating microwave fast-passage during continuous optical pumping. Under conditions that the SLR processes can be ignored, and the ISC rates are independent of the triplet population, the method yields the decay constants for emission in a particular vibronic band, the steady-state populations, and the relative ISC rate constants. In many cases, the assumptions are not valid. In particular, SLR usually can not be ignored even at 1·3 K for triplet states which have sublevel decay constants the order of one sec [13]. Also, under strong optical pumping of a dilute system with a long triplet lifetime, the steady state populations of the phosphorescent state and the ground singlet state may be comparable or even inverted. The ISC rates then depend upon the triplet state population and will vary during the transient induced by microwave saturation. In this section we give approximate expressions for the time-dependence of the sublevel populations following the saturation of a pair of levels during continuous optical pumping. Schwoerer and Sixl [20] have given exact expressions for the time-dependence of the sublevel populations under several experimental conditions. Although their equations include SLR and variable ISC, they are only valid in the high-field approximation, and thus cannot be applied to zero-field measurements.

The time-dependence of the populations of the triplet sublevels is given by solutions to the three differential equations, a representative being

$$dn_u/dt = K_u' n_s' - (k_u + k_{uv} + k_{uw}) n_u + k_{vu} n_v + k_{wu} n_w, \tag{4}$$

where n_s' is the population of the excited singlet state from which ISC is assumed to occur. Under conditions of strong optical pumping on a dilute system, $n_s' \propto n_s \simeq n_0 - n_t$, where n_0 is the total number of molecules being observed, n_t being in the phosphorescent state and n_s in the ground state. Substituting this expression for n_s' in equation (4) we obtain

$$d\Delta n_u/dt = -\rho_u \Delta n_u + (k_{vu} - K_u)\Delta n_v + (k_{wu} - K_u)\Delta n_w, \tag{5}$$

where

$$\Delta n_u = n_u - n_u{}^0, \quad \rho_u = \rho_u' + K_u, \quad \text{and} \ldots K_u \propto K_u'.$$

If $|k_{uv}-K_u| < |\rho_v-\rho_u|$, then the following equation is obtained in first-order for the time-dependence of the population of T_u following the saturation of a pair of levels, T_u and T_v, at $t=0$.

$$\Delta n_u{}^{(1)}(t)=(\tfrac{1}{2})(n_v{}^0-n_u{}^0)[q_{uv}\exp(-\rho_u t)-(k_{vu}-K_u) \times \exp(-\rho_v t)]/(\rho_u-\rho_v). \quad (6)$$

Saturation of T_v and T_w at $t=0$ gives

$$\Delta n_u{}^{(1)}(t)=(\tfrac{1}{2})(n_v{}^0-n_w{}^0)\left\{\frac{(k_{vu}-K_u)}{(\rho_u-\rho_v)}[\exp(-\rho_u t) - \exp(-\rho_v t)]-\frac{(k_{wu}-K_u)}{(\rho_u-\rho_w)}[\exp(-\rho_u t)-\exp(-\rho_w t)]\right\}. \quad (7)$$

In equation (6), $q_{uv}=(\rho_u-\rho_v)+(k_{vu}-K_u)$. In saturating a single pair of sublevels at $t=0$, the populations of the saturated levels will follow equation (6), whereas the population of the level not pumped by the microwaves will follow equation (7). The characteristic of the unpumped level is that $\Delta n_u(0)=0$, whereas the characteristic of a pumped level is that $\Delta n_u(0)=-\Delta n_v(0)\neq 0$ (unless their steady-state populations happen to be accidentally equal). The effect on the steady state phosphorescence intensity of the mth vibronic band is obtained from equations (6) and (7) by multiplying by the appropriate radiative rate constants along the crystal direction under observation.

$$\Delta I_m(t)=s\sum_u k_{u,\,m}{}^{\mathrm{r}}(\mathbf{p})\Delta n_u(t). \quad (8)$$

In equation (8), s is a proportionality constant, and $k_{u,\,m}{}^{\mathrm{r}}(\mathbf{p})$ is the radiative rate constant for emission in the mth vibronic band from the T_u sublevel along the observation direction represented by the vector $\mathbf{p}$.

4.2. *Results*

The phosphorescence transients which occur upon saturating the three zero-field transitions while monitoring either the 0,0-band or the 0,0–262 cm^{-1} band of 2,3-dichloroquinoxaline in durene are given in figure 5. Saturation of the $T_y \leftrightarrow T_z$ transition while monitoring the 0,0-band emission is given in figure 5 (*a*). Microwave saturation is accompanied by a sudden increase in the emission which decays with a simple exponential decay characteristic of the T_z sublevel. The ratio of the transient to the steady state phosphorescence intensity of the 0,0-band is related to the steady-state populations of the T_y and T_z levels. The ratio is simply

$$\Delta I_0{}^{yz}/I_0=(n_y{}^0-n_z{}^0)(1-S)/2(n_z{}^0+Sn_y{}^0)$$

assuming (*vide infra*) $k_{x,\,0}{}^{(\mathrm{r})}(\mathbf{p})=0$, and with $S=k_{y,\,0}{}^{(\mathrm{r})}(\mathbf{p})/k_{z,\,0}{}^{(\mathrm{r})}(\mathbf{p})$. S was obtained previously from the flash excitation experiments. When the 0,0–262 cm^{-1} band is monitored while saturating the $T_y \leftrightarrow T_z$ transition a decrease in the steady state intensity is seen (figure 5 (*d*)) which decays exponentially with a time constant characteristic of T_y. Since neither the T_z nor T_x sublevel is found to be radiative in the 0,0–262 cm^{-1} band, the ratio of the transient to the steady state intensity is

$$\Delta I_{262}{}^{yz}/I_{262}=(n_z{}^0-n_y{}^0)/2n_y{}^0.$$

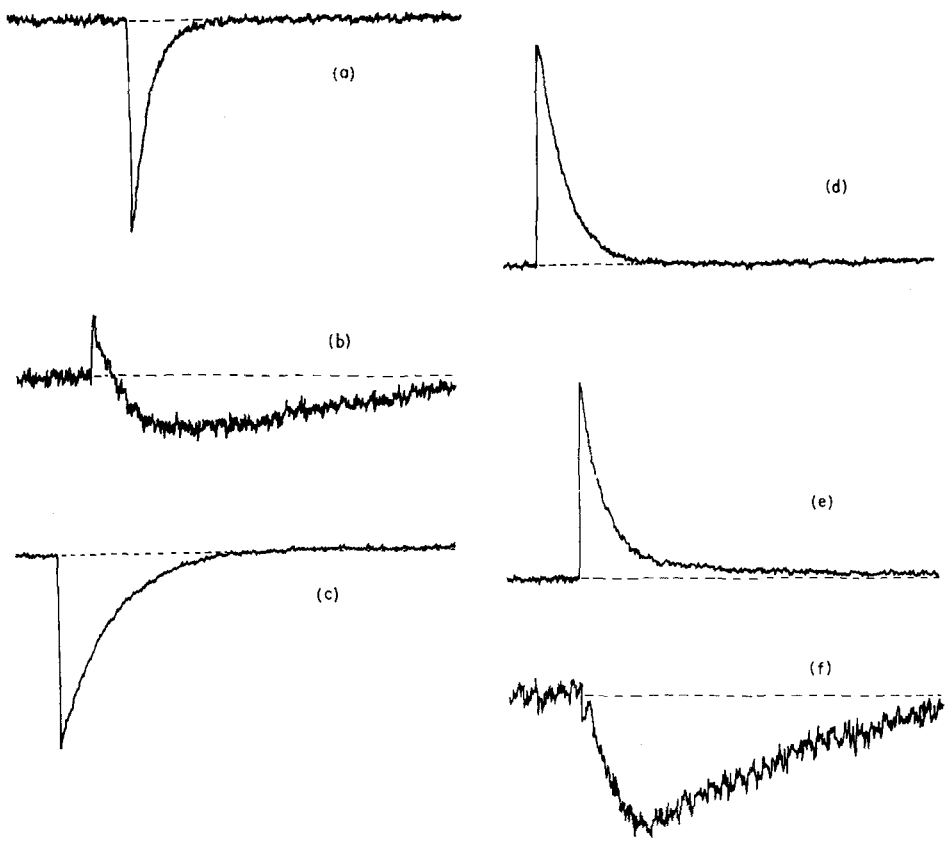

Figure 5. Phosphorescence transients induced by saturating microwave fast-passages during continuous optical pumping. Emission increases downwards. Sample is 2,3-dichloroquinoxaline in durene. (*a*) 0,0–band emission saturating the $T_y \leftrightarrow T_z$ microwave transition. $T = 1{\cdot}3$ K. Time base = 5·0 sec. (*b*) 0,0–band emission saturating the $T_y \leftrightarrow T_x$ microwave transition. $T = 4{\cdot}2$ K. Time base = 2·5 sec. (*c*) 0,0–band emission saturating the $T_z \leftrightarrow T_x$ microwave transition. $T_1 = 1{\cdot}3$ K. Time base = 2·5 sec. (*d*) 0,0–262 cm^{-1}–band emission saturating the $T_y \leftrightarrow T_z$ microwave transition. $T = 1{\cdot}3$ K. Time base = 2·5 sec. (*e*) 0,0–262 cm^{-1}–band emission saturating the $T_y \leftrightarrow T_x$ microwave transition. $T = 1{\cdot}3$ K. Time base = 2·5 sec. (*f*) 0,0–262 cm^{-1}–band emission saturating the $T_z \leftrightarrow T_x$ microwave transition. $T = 1{\cdot}3$ K. Time base = 5·0 sec.

Similar expressions are obtained for the steady state populations of T_x and T_z by monitoring the 0,0-band emission while saturating the $T_x \rightarrow T_z$ transition (figure 5 (*c*)) and for the steady state populations of T_x and T_y from monitoring the 0,0–262 cm^{-1} band while saturating the $T_x \leftrightarrow T_y$ transition (figure 5 (*e*)). These four measurements are sufficient to over-determine the relative steady-state populations of the three sublevels. The results at both 1·3 and at 4·2 K are reported in the table. At both temperatures, $n_y^0 > n_x^0 > n_z^0$. We always find a long exponential tail following the fast decay component in figure 5 (*e*), although its relative intensity depends upon the experimental conditions. The decay constant is that of the T_x sublevel. Since it represents a *decrease* in the steady-state phosphorescence intensity, it cannot represent emission from the T_x sublevel

(which becomes overpopulated after saturation with T_y). We interpret the long tail to be caused by under-population of T_y due to a decrease in the ISC rate after saturation of the populations of T_y and T_x. Equation (6) predicts a component of Δn_y which has a decay constant ρ_x and which looks like

$$\Delta n_y(t > \rho_y^{-1}) \approx \frac{(n_y^0 - n_x^0)}{2(\rho_y - \rho_x)} (k_{xy} - K_y) \exp(-\rho_x t).$$

It will be negative (as observed) as long as $K_y > k_{xy}$. The observation of an exponential tail with a negative pre-exponential term implies that under our experimental conditions ISC to T_y has a larger rate constant than SLR between T_x and T_y. We can predict that the relative amplitude of the exponential tail decreases under weaker optical pumping and vanishes when $K_y = k_{xy}$. It also follows that at higher T, as k_{xy} increases, the amplitude of the long tail should decrease. We have observed this effect by raising the temperature to 4·2 K.

Saturation of the $T_x \leftarrow T_z$ transition while monitoring the phosphorescence in the 0,0–262 cm^{-1} band is shown in figure 5 (*f*). Very little if any discontinuous break in the intensity is seen at $t = 0$, which indicates that neither T_x nor T_z is radiative in the 0,0–262 cm^{-1} vibronic band. The phosphorescence transient should then follow the population of T_y as given by equation (7). The initial portion of the transient is complex, given by a combination of exponential terms with rate constants ρ_y and ρ_z, which has not been analyzed due to the poor signal-to-noise ratio. The long exponential tail decays with the rate constant ρ_x, and represents an increase in the normal T_y emission. Equation (7), for $t \gg \rho_y^{-1}, \rho_z^{-1}$, gives

$$\Delta n_y(t \gg \rho_z^{-1}) \approx \frac{(n_x^0 - n_z^0)}{2(\rho_y - \rho_x)} (K_y - k_{xy}) \exp(-\rho_x t).$$

Since $(n_x^0 - n_z^0)$ and $(\rho_y - \rho_x)$ are both positive, the sign of the pre-exponential part of the tail is positive (as observed) if $K_y > k_{xy}$. This is consistent with the explanation of the long negative tail on the 0,0–262 cm^{-1} band which occurs on saturating the $T_y \leftrightarrow T_x$ transition.

Saturation of the $T_y \leftrightarrow T_x$ transition while monitoring the 0,0–262 cm^{-1} band gives rise to the phosphorescence transient shown in figure 5 (*b*). The discontinuous decrease in the intensity observed at $t = 0$ shows that T_y is radiative in the 0,0-band in agreement with the flash experiments. The initial jump decays as the sum of two exponential terms, one with decay constant ρ_y, and a slower one with decay constant ρ_x. The pre-exponential terms are of opposite sign, which is consistent with either (*a*) a small amount of radiation originating from the T_x sublevel, or (*b*) radiation from the T_z sublevel whose population in this experiment would be given by equation (7). At long t, equation (7) gives the time dependence of Δn_z as

$$\Delta n_z(t \gg \rho_z^{-1}) \approx \frac{(n_y^0 - n_x^0)}{2(\rho_z - \rho_x)} (k_{xz} - K_z) \exp(-\rho_x t).$$

The pre-exponential term is positive if $k_{xz} > K_z$. Since $K_z \approx (\frac{1}{8}) K_y$, this is not an unreasonable explanation for the appearance of the long exponential tail. At higher temperatures k_{xz} will increase, and we predict that the amplitude of the long exponential tail will increase relative to the initial transient if it represents

mainly emission from T_z via SLR from T_x. Figure 5 (*b*), in fact, represents an experiment made at 4·2 K. At lower temperature (1.35 K) the amplitude of the long tail is barely discernible and the phosphorescence transient consists almost entirely of the fast component. This proves that the long component of the transient is due to emission from T_z whose population is affected by SLR from T_x.

The bands of Type III, which occur at 0,0–311 and 0,0–490 cm^{-1} in 2,3-dichloroquinoxaline in durene are of mixed polarization, and contain comparable emission from T_y and T_z. As was discussed earlier, the crystal structure of the durene host is such that x-polarized and z-polarized emission will have the same spatial polarization. Consequently, the relative intensities of the 0,0 (Type I) and 0,0–262 cm^{-1} (Type II) bands will be independent of the crystal orientation, whereas the y-polarized component of the Type III bands should vary relative to the z-polarized component as the crystal is rotated. Figure 2 (*b*) and (*d*) show the phosphorescence transient observed in the 0,0–490 cm^{-1} band upon saturating the $T_y \leftrightarrow T_z$ microwave transition for the two different crystal orientations. The orientations are the same as those for figure 2 (*a*) and (*c*) respectively. No polarizers were used either for the observation of the phosphorescence spectra or the ODMR phosphorescence transients. The differences are attributable to the difference in the spatial polarization of the two components (T_y origin, and T_z origin) of the Type III bands. The phosphorescence responses of figures 2 (*b*) and (*d*) each consist of the superposition of two exponential decays, one with decay constant ρ_y with a negative pre-exponential term and the other with the smaller decay constant ρ_z having a positive pre-exponential term. Clearly, both sublevels are radiative in agreement with the assignment of 0,0–490 cm^{-1} as a Type III band. The 0,0–311 cm^{-1} band shows similar signals and the same orientation dependence. The different appearance of the ODMR signals in figures 2 (*b*) and (*d*) is due to the difference in the relative radiative rate constants along the two directions of observation. In the orientation corresponding to figures 2 (*c*) and (*d*), the T_y sublevel is more radiative than the T_z sublevel in Type III bands, whereas in the other orientation, almost all the emission originates from the T_z sublevel. In the orientation represented by figures 2 (*a*) and (*b*), the crystal is observed along the b-axis, which is nearly along the y-axis of the durene molecules, and consequently a direction of minimum radiation for y-polarized emission. The spectra of figures 2 (*c*) and (*d*) are collected along a crystal direction normal to the b-axis along which y-polarized emission is a maximum.

5. 1,2,4,5-Tetrachlorobenzene host

5.1. *Results*

The experiments outlined in the previous sections were carried out on 2,3-dichloroquinoxaline as a substitutional impurity in single crystals of 1,2,4,5-tetrachlorobenzene. The results were basically similar with the following differences being the most notable. The lifetimes of each of the spin sublevels is reduced in the tetrachlorobenzene host crystal. The lifetimes at 1·3 K are found to be $\rho_x^{-1} = 1{\cdot}3 \pm 0{\cdot}2$ sec, $\rho_y^{-1} = 0{\cdot}125 \pm 0{\cdot}005$ sec, and $\rho_x^{-1} = 0{\cdot}175 \pm 0{\cdot}01$ sec. The radiative patterns to Type I and Type II bands are found to be the same as in the durene host, but instead of the Type III bands with comparable radiative intensity from T_y and T_z, only emission from T_y is found in tetrachlorobenzene.

6. Discussion of results

We have measured the effects of saturating microwave fast passages on the decay of the phosphorescence of 2,3-dichloroquinoxaline following flash excitation as well as during continuous optical pumping. The former technique is useful for obtaining in a direct manner the relative ISC rates to the individual sublevels since the effects of spin-lattice relaxation are minimized. The details of the transient responses of the phosphorescence emission to microwave saturation can be understood only if the effects of SLR, the effect of the triplet population on ISC, and the spatial polarization of the radiation are included. These effects have been observed and explained with the help of first order solutions of the rate equations.

It is found that SLR is important in determining the steady state populations of the triplet sublevels at temperatures as low as 1·3 K. In the absence of SLR, the steady-state populations should be given by $n_u^0 = p_u/\rho_u'$, where the p_u are obtained from the flash excitation measurements. The predicted steady-state populations are given in the last column of the table. Comparison with the populations obtained from the continuous optical pumping experiments shows that there is a predominant $T_x \rightarrow T_z$ relaxation pathway.

We have established by flash excitation experiments that the principal ISC route populates the T_y sublevel, in agreement with earlier conclusions from steady-state measurements [4]. A secondary ISC route populates T_z to the extent of about 10 per cent. T_y decays primarily by radiation to vibronic levels of a_2 and b_1 symmetry, although a small amount of radiative activity is found in the 0,0-band. This could be explained by the reduction of the molecular symmetry below C_{2v} by the crystal field in durene. T_z decays by radiation in the 0,0-band and totally symmetric vibronic bands. It also emits to vibronic states of b_1 symmetry in durene, but not in tetrachlorobenzene host crystals.

As mentioned in § 2.1, there is no group theoretical reason why emission to a_2 and b_1 vibronic bands should not occur from both T_y and T_z ,and consequently there is no fundamental distinction between Type II and Type III bands. The reason that T_z is not found to be radiative to a_2 vibronic bands may be a consequence of the relative magnitudes of the pertinent spin-orbit matrix elements, i.e.,

$$\langle {}^1B_2 | \mathscr{H}_{\mathrm{so}}{}^{(z)} | {}^3B_1 \rangle \ll \langle {}^1A_1 | \mathscr{H}_{\mathrm{so}}{}^{(y)} | {}^3B_1 \rangle.$$

We suggest that the lack of b_1 vibronic emission from T_z in 1,2,4,5-tetrachlorobenzene is a consequence of selective spin-orbit coupling routes, i.e.

$$\langle {}^1A_1 | \mathscr{H}_{\mathrm{so}}{}^{(z)} | {}^3A_2 \rangle \ll \langle {}^1B_2 | \mathscr{H}_{\mathrm{so}}{}^{(y)} | {}^3A_2 \rangle,$$

and that a different mechanism is responsible for b_1 emission from T_z in durene. In quinoxaline, the lowest singlet is ${}^1B_1(n, \pi^*)$, whereas this state is blue-shifted and the ${}^1A_1(\pi, \pi^*)$ is red-shifted by halogen substitution. Tinti and El-Sayed suggest [14] that the origin of ${}^1A_1$ is shifted below that of ${}^1B_1$ in 2,3-dichloroquinoxaline. If this is the case, a large mixing of the ${}^1A_1$ and ${}^1B_1$ electronic states could result from a breakdown of the adiabatic approximation [21]. The mixing of these electronic states would be particularly sensitive to solvent perturbations since the adiabatic approximation will only fail if the Born–Oppenheimer energies of the ${}^1B_1$ origin and a b_1 vibronic level of ${}^1A_1$ become nearly coincident. In durene, then, we propose that the ${}^1B_1$ origin is admixed with a vibronic level of ${}^1A_1$ which has B_1 vibronic symmetry. First order spin-orbit coupling between the T_z

sublevel of $^3B_2$ and this non-Born–Oppenheimer state results in both the 0,0–emission [22] and the b_1 vibronic emission.

We wish to thank Dr. Christopher J. Winscom for first suggesting to us the anisotropic spatial distribution of polarized emission from single crystals. We are grateful to the National Science Foundation and the National Institutes of Health for their support.

References

[1] Sharnoff, M., 1967, *J. chem. Phys.*, **46,** 3263.
[2] Kwiram, A. L., 1967, *Chem. Phys. Lett.*, **1,** 272.
[3] Schmidt, J., and Van der Waals, J. H., 1968, *Chem. phys. Lett.*, **2,** 640.
[4] Tinti, D. S., El-Sayed, M. A., Maki, A. H., and Harris, C. B., 1969, *Chem. Phys. Lett.*, **3,** 343.
[5] El-Sayed, M. A., Owens, D. V., and Tinti, D. S., 1970, *Chem. Phys. Lett.*, **6,** 395.
[6] Harris, C. B., Tinti, D. S., El-Sayed, M. A., and Maki, A. H., 1969, *Chem. Phys. Lett.*, **4,** 409. Chan, I. Y., Schmidt, J., and van der Waals, J. H., 1969, *Chem. Phys. Lett.*, **4,** 269. Buckley, M. J., Harris, C. B., and Maki, A. H., 1970, *Chem. Phys. Lett.*, **4,** 591. Cheng, L. T., van Zee, T. A., and Kwiram, A. L., 1970, *Bull. Am. phys. Soc.*, **15,** 268, 373.
[7] Kuan, T. S., Tinti, D. S., and El-Sayed, M. A., 1969, *Chem. Phys. Lett.*, **4,** 507.
[8] Schmidt, J., Veeman, W. S., and van der Waals, J. H., 1969, *Chem. Phys. Lett.*, **4,** 341.
[9] Antheunis, D. A., Schmidt, J., and van der Waals, J. H., 1970, *Chem. Phys. Lett.*, **6,** 255.
[10] Harris, C. B., 1971, *J. chem. Phys.*, **54,** 972.
[11] Harris, C. B., and Hoover, R. J., 1972, *J. chem. Phys.*, **56,** 2199.
[12] Winscom, C. J., and Maki, A. H., 1971, *Chem. Phys. Lett.*, **12,** 264.
[13] Schmidt, J., Antheunis, D. A., and van der Waals, J. H., 1971, *Molec. Phys.*, **22,** 1.
[14] Tinti, D. S., and El-Sayed, M. A., 1971, *J. chem. Phys.*, **54,** 2529.
[15] Hutchison, C. A., Jr., and Mangum, B. W., 1961, *J. chem. Phys.*, **34,** 908.
[16] Robertson, J. M., 1933, *Proc. R. Soc.* A, **141,** 594.
[17] Dean, C., Pollak, M., Graven, B. M., and Jeffrey, G. A., 1958, *Acta crystallogr.*, **11,** 710.
[18] Monfils, A., 1955, *C. r. hebd. Séanc. Acad. Sci., Paris,* **241,** 561 ; Herbstein, F. H., 1965, *Acta crystallogr.*, **18,** 997.
[19] El-Sayed, M. A., and Olmsted, J., III, 1971, *Chem. Phys. Lett.*, **11,** 568.
[20] Schwoerer, M., and Sixl, H., 1969, *Z. Naturf.* A, **24,** 952.
[21] Messiah, A., 1962, *Quantum Mechanics*, Vol. II (North-Holland Publishing Co.), p. 786.
[22] van der Waals, J. H., and de Groot, M. S., 1967, *The Triplet State*, edited by A. B. Zahlan (Cambridge University Press), p. 101.